

# Carbon isotope ( $\delta^{13}\text{C}_{\text{carb}}$ ) heterogeneity in deep-water Cambro-Ordovician carbonates, western Newfoundland

Sara B. Pruss <sup>a,\*</sup>, Katherine A. Castagno <sup>b</sup>, David A. Fike <sup>c</sup>, Matthew T. Hurtgen <sup>d</sup>

<sup>a</sup> Department of Geosciences, Smith College, Northampton, MA 01063, USA

<sup>b</sup> Department of Geology & Geophysics, Woods Hole Oceanographic Institution, Woods Hole, MA 02543, USA

<sup>c</sup> Department of Earth and Planetary Science, Washington University, St. Louis, MO 63130-4899, USA

<sup>d</sup> Department of Earth and Planetary Sciences, Northwestern University, Evanston, IL 60208, USA



## ARTICLE INFO

### Article history:

Received 11 March 2015

Received in revised form 25 September 2015

Accepted 1 October 2015

Available online 9 October 2015

### Keywords:

Cow Head Group

Cambrian

Conglomerate

Laurentia

## ABSTRACT

Carbonates of western Newfoundland span the Cambro-Ordovician interval and preserve a record of slope-basinal deposition in the Cow Head Group near Cow Head. This unit consists of conglomerates and ribbon and laminated limestone interbedded with shale that is well exposed in sea cliffs at Cow Head Peninsula. These conglomerates, although prevalent throughout the section, vary in thickness and abundance stratigraphically and record both local disruption and large-scale episodic sedimentation events. Microfacies drilled for carbon isotope ( $\delta^{13}\text{C}_{\text{carb}}$ ) analysis of conglomerates reveal isotopic heterogeneity within individual samples, in some cases more than 1‰. While this might be an expected outcome of drilling multiple areas of a heterogeneous conglomerate hand sample, permil-level variability was observed both between individual clasts in a sample, between different parts of the same matrix, and between a clast and its surrounding matrix. No associated variation in  $\delta^{18}\text{O}_{\text{carb}}$  or trace element distributions exists to suggest that this  $\delta^{13}\text{C}_{\text{carb}}$  variability is the result of later-stage meteoric diagenesis. The  $\delta^{13}\text{C}_{\text{carb}}$  variability suggests multiple sources of dissolved inorganic carbon (DIC) associated with carbonate precipitation for phases within these individual samples. These data indicate that processes such as local organic matter remineralization and early authigenic carbonate precipitation during lithification at the sediment–water interface (SWI) are either contributing to or controlling  $\delta^{13}\text{C}_{\text{carb}}$  values in Cambrian carbonates, perhaps more so than at other intervals in Earth history.

© 2015 Elsevier B.V. All rights reserved.

## 1. Introduction

Carbon isotope values have long been used to reconstruct paleoenvironmental conditions ranging from organic carbon burial (e.g., Arthur et al., 1988; Sackett, 1991; Hayes et al., 1999) to partial pressure of CO<sub>2</sub> (Popp et al., 1989; Freeman and Hayes, 1992) to, more recently, an approximation of the sink of carbonate carbon precipitated on the seafloor through remineralization processes (Schrag et al., 2013). Despite the wide use of carbon isotopes as proxies for ancient environments and their utility in providing chemostratigraphic linkages between ancient strata (e.g., Knoll et al., 1986; Hayes et al., 1999), substantial debate still surrounds the meaning of these values and the timing of their origins (e.g., Grotzinger et al., 2011). A  $\delta^{13}\text{C}$  signal in the marine dissolved inorganic carbon (DIC) reservoir is often interpreted as reflecting the balance between the flux and isotopic composition of the major sources to and from the ocean (Kump and Arthur, 1999), but ascertaining the timing of the incorporation of  $\delta^{13}\text{C}$  signals in carbonate sediments and sedimentary rocks – and the local processes

that may affect their composition (e.g., Oehlert and Swart, 2014) – is critical before any paleoenvironmental interpretation can be made.

In western Newfoundland, carbonate and siliciclastic strata straddle the Cambrian and Ordovician periods (e.g., Chow and James, 1987; Cowan and James, 1993) and record the biotic and environmental change that preceded and spanned the largest biotic diversification in the history of life, the Ordovician radiation (e.g., Droser and Finnegan, 2003). Previous work has shown  $\delta^{13}\text{C}_{\text{carb}}$  oscillations through middle and later Cambrian shallow-water sections of Newfoundland, including a large (~4‰) positive excursion known as the SPICE event (Steptoean positive isotopic excursion; Saltzman et al., 2000, 2004; Hurtgen et al., 2009). However, little isotope data exist on deep-water sections, like the Cow Head Group exposed near Cow Head, Newfoundland (Fig. 1). The composition of the Cow Head – turbidites and fine-grained carbonates – suggests background sedimentation punctuated by local reworking and episodic mass flow from shallower environments. Some large-scale debris flows delivered both unconsolidated carbonates and variably lithified clasts to the deeper waters. Thus, the resulting deep-water strata contain carbonate sourced both locally and from shallower locations, recording a complex diagenetic history during lithification (Sucheki and Hubert, 1984; Coniglio and James, 1990). Carbon isotope analysis of clasts and fine-grained matrix of the Cow Head

\* Corresponding author. Tel.: +1 413 585 3948.

E-mail address: [spruss@smith.edu](mailto:spruss@smith.edu) (S.B. Pruss).

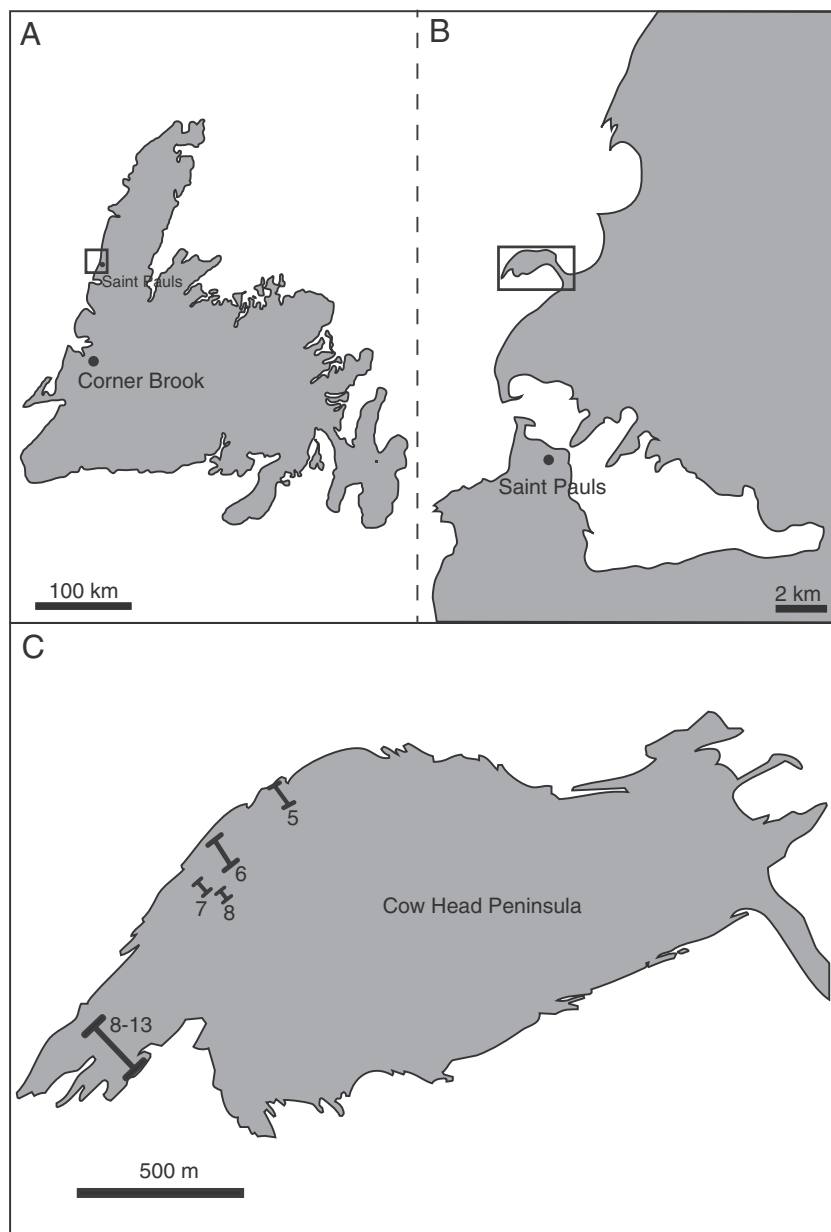


**Fig. 1.** Locality map. A) Newfoundland, B) inset from A showing Cow Head Peninsula; and C) inset from B showing location of measured sections for Beds 5 to 13 along Cow Head Peninsula.

Group can reveal the origins of these carbonate components, as well as the timing of lithification and other early diagenetic processes. Here, we aim to understand the processes that impart the carbon isotope signals on Cow Head carbonate strata and to evaluate the potential for (variably transported) deep-water strata to record global marine  $\delta^{13}\text{C}_{\text{carb}}$  signals. In addition,  $\delta^{13}\text{C}_{\text{carb}}$  variability between these carbonate phases can shed light on the contribution of authigenic carbonate precipitation to the enhanced apparent lateral and stratigraphic variability in  $\delta^{13}\text{C}_{\text{carb}}$  signals at this time.

## 2. Geological setting

### 2.1. Overview

The Cambro-Ordovician Cow Head Group at the Cow Head Peninsula (Fig. 1) is comprised of the Shallow Bay Formation, which includes the Downes Point Member, the Tuckers Cover Member, the Stearing Island Member, and the Factory Cove Member (e.g., James and Stevens, 1986; Zhang and Barnes, 2004). Estimates suggest that the unit represents

approximately 70 million years of deposition in a deep-water slope setting (James and Stevens, 1986). It is more than 350-m-thick at the Cow Head Peninsula and consists of carbonate-rich conglomerate, shale and limestone that span the Middle Cambrian through the Middle Ordovician (e.g., James and Stevens, 1986; Zhang and Barnes, 2004; Azmy et al., 2014; Tripathy et al., 2014). Shale and limestone are interbedded, and conglomerate beds range from massive (clasts greater than 5 m in diameter) to smaller lenticular units consisting of cm- to dm-sized intraclasts. James and Stevens (1986) divide the Cow Head Peninsula into a system of 15 beds based on lithofacies, but only Beds 5 through 13 were investigated in this study.

### 2.2. Biostratigraphic constraints on the Cow Head Group

The Cow Head Group has been widely studied with regard to its biostratigraphically useful fossils, in part because it correlates to strata that preserve the GSSP for the Cambro-Ordovician boundary at nearby Green Head. In particular, conodonts, graptolites and trilobites have been examined in some detail in previous work on this section (Fig. 2;

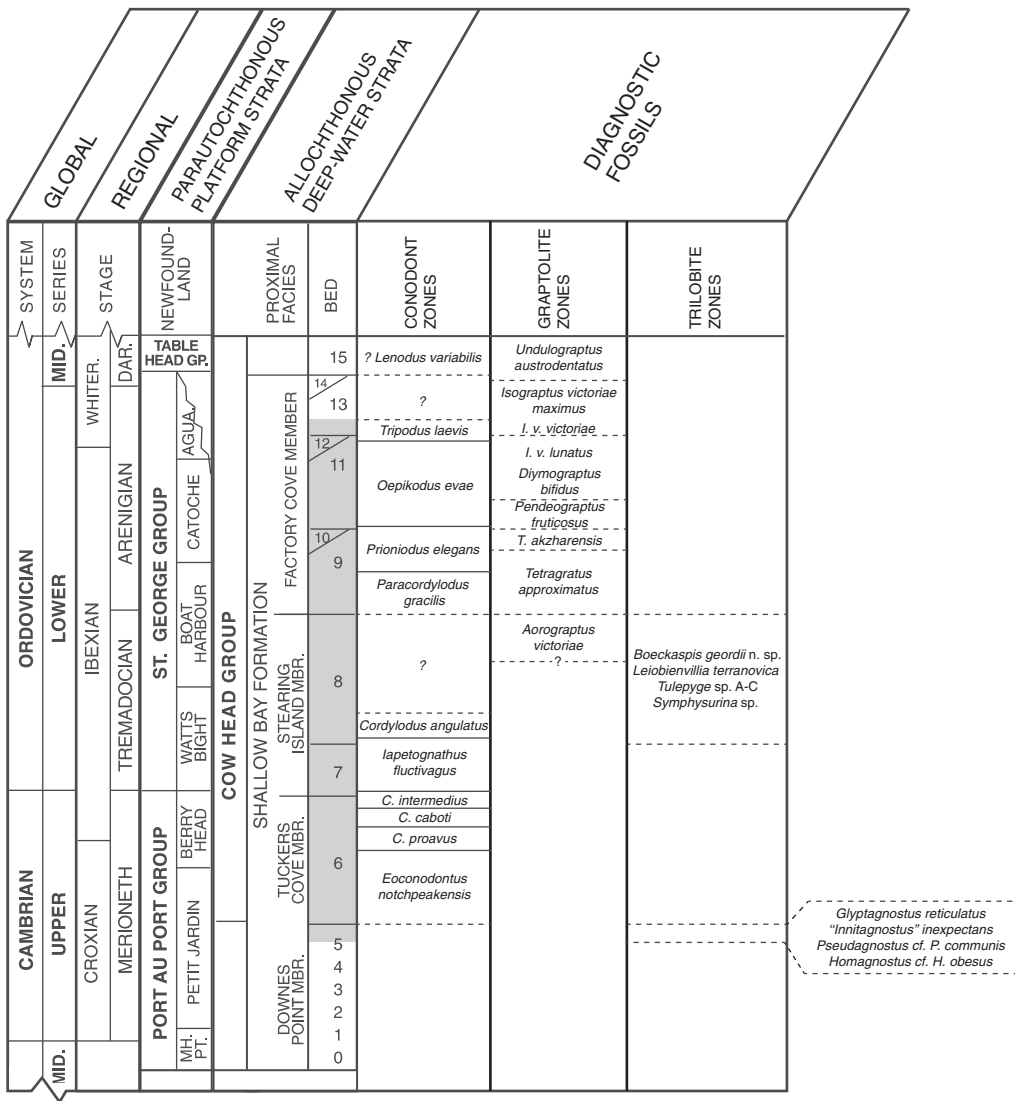


**Fig. 2.** Diagram showing age constraints and correlations of the Cow Head Group to nearby shallow-water equivalent sections (modified from Zhang and Barnes, 2004). Biostratigraphic age constraints are provided here from conodonts and graptolites (Zhang and Barnes, 2004) and trilobites (Westrop and Eoff, 2012; Karim, 2008). Gray shaded area shows portion of the Cow Head Group sampled in this work.

Zhang and Barnes, 2004; Karim, 2008; Westrop and Eoff, 2012). Because much of the Cow Head Group consists of allochthonous carbonate deposits, biostratigraphically useful fossils have been extracted both from clasts of conglomerate that were likely transported and interbedded shales that record deep water deposition. Bed 5 has few diagnostic fossils, but it does preserve an important trilobite assemblage (Westrop and Eoff, 2012). Here, from boulders preserved in Bed 5, the *Innitagnostus inexpectans* Fauna of Newfoundland is thought to record an early occurrence of *Dunderbergia* in the *Aphelaspis* Zone. This trilobite zone occurs at the time of the SPICE event in Newfoundland shelfal equivalent sections (Saltzman et al., 2004; Hurtgen et al., 2009), suggesting that the strata of Bed 5 should preserve the SPICE event or were deposited just after, perhaps during reworking of shelfal clasts into deeper-water sections.

The rest of the Cow Head Group at Cow Head is fairly well constrained from conodont and graptolite biostratigraphy. Conodont zones of Bed 6 and Bed 7 suggest a Furongian (upper Cambrian) age (e.g., *Eoconodontus notchpeakensis*; Zhang and Barnes, 2004), although the boundary between the Cambrian and Ordovician remains problematic at this site (e.g., Karim, 2008). A trilobite fauna recovered from Bed 8 in concert with diagnostic conodonts suggest an Early Ordovician age for this part of the section (Karim, 2008; Zhang and Barnes, 2004).

Beds 9 through 13 also record deposition during the Early Ordovician, though the boundary between the Tremadocian and Floian (Arenigian) is not well constrained (e.g., Zhang and Barnes, 2004).

### 2.3. Field observations

At the base of our measured section, upper Bed 5 is part of the Downes Point Member and constrained biostratigraphically to Furongian Cambrian (Steptoean) strata (Zhang and Barnes, 2004; James and Stevens, 1986; Fig. 2). A seventeen-meter-thick portion of upper Bed 5 was measured and sampled at Cow Head. Facies consist predominantly of conglomerate with micrite-rich matrix (Fig. 3A). The contact between Bed 5 and Bed 6 is marked by the appearance of quartz-rich sand matrix (James and Stevens, 1986), but we observed a gradual transition from micrite-rich to quartz-dominated with minor micrite matrices in samples ~10 m below the contact between Bed 5 and Bed 6. Bed 6 is part of the Tuckers Cover Member and is constrained biostratigraphically to Furongian Cambrian (Sunwaptan) strata. We measured approximately 55 m of Bed 6 at Cow Head; facies were predominantly thinly bedded limestone and conglomerates with micritic and quartz-rich matrices (Fig. 3B). Zhang and Barnes (2004) place the Cambro-Ordovician boundary at the contact between Beds 6 and 7 in

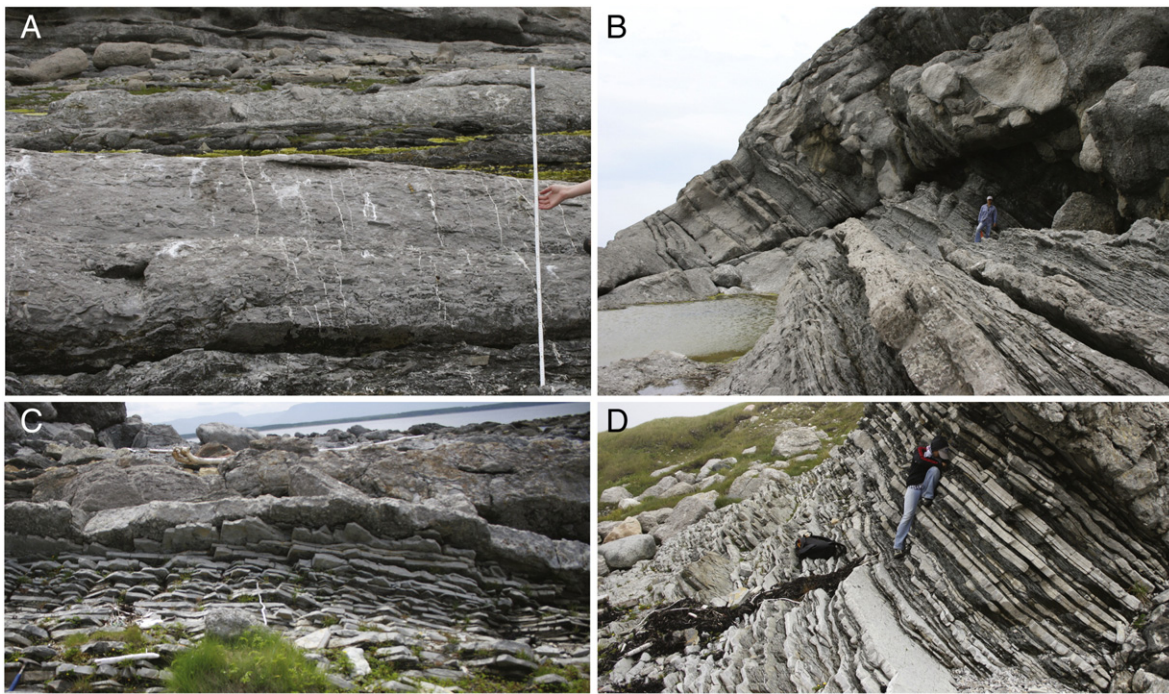


**Fig. 3.** Field photographs of Beds 5, 6, 7, 8 and 9 showing conglomerates and thinly bedded limestone from each unit. A) Massive limestone conglomerates of Bed 5 with fine-grained carbonate matrix, meter stick for scale; B) Thin limestone beds and lenticular conglomerates of upper Bed 6 in contact with massive welded conglomerates of Bed 7. C) Alternating thin limestone beds and shale of upper Bed 9 capped by lenticular conglomerates of Bed 9, hammer in lower left corner for scale; E) Upper Bed 9 overlain by conglomeratic Bed 10 (visible in upper right corner).

correlative, continuous sections at Green Point (Green Point Global Boundary Stratotype Section and Point; Barnes, 1988; Johnston and Barnes, 1999; Cooper et al., 2001), although a major erosive surface exists at the base of Bed 7 at Cow Head (Fig. 3B; James and Stevens, 1986).

Beds 7 and 8 are both part of the Stearing Island Member. Bed 7 overlies Bed 6 and is constrained biostratigraphically to the Tremadocian (Lowermost Ordovician) (Zhang and Barnes, 2004). We measured approximately 20 m of Bed 7 at Cow Head, and facies consisted of large, distinct conglomeratic beds with massive boulder-sized clasts (Fig. 3B). Bed 8 is Lower Ordovician Tremadocian to Floian (Arenigian) in age (Zhang and Barnes, 2004), and approximately 40 m of Bed 8 is exposed at Cow Head. It is heavily faulted and consists of three major facies packages: a lower unit of thinly bedded limestone and conglomerate, a middle unit of massive conglomerate with boulder-sized clasts, and an upper unit of thinly bedded limestone and conglomerate.

Beds 9 through 13 are part of the Factory Cove Member. About 52 m of Bed 9 is exposed at Cow Head, and it is Floian (Arenigian) in age (Zhang and Barnes, 2004). Bed 9 consists of thinly bedded limestone and rare conglomerate with a shale-rich base (Fig. 3C and D). About 20 m from the base of Bed 9, ~10 m of this unit is covered by beach and was not sampled. Bed 10 is approximately 1.7 m and consists of a single, massive conglomerate (Fig. 3D). Bed 11 consists of alternating beds of silicified and fissile shale, with dolomitic beds increasing in the upper half of the unit. We measured approximately 18 m of Bed 11. Bed 12 consists of a massive conglomerate approximately 10 m in thickness. Bed 13 (Early Ordovician; Zhang and Barnes, 2004) is heavily faulted and consists of approximately 20 m of thinly bedded limestone. Conglomerates were sampled from all beds except Bed 11.

### 3. Methods

Two hundred and sixty-seven carbonate samples were collected and drilled from Bed 5 through Bed 13 at meter-scale. Carbonate lithologies included fine-grained carbonate facies, grainstone, dolostone, and

conglomerate. When constructing the isotopic profile for the Cow Head, conglomerates were generally avoided except in the cases of Beds 5, 7 and 8 where the entire bed was composed of conglomerate. In those cases, matrix was typically drilled from conglomerate samples. However, in a few areas only clasts could be sampled and drilled (34 samples of clast out of 267 drilled; Fig. 4).

In addition to the bulk carbon measured for the isotopic profile, a subset of 51 conglomerates that span the Cow Head Group from Beds 5 to 13 was cut and drilled in multiple places to ascertain isotopic heterogeneity of individual microfacies. Note that since conglomerate samples were generally avoided in the construction of the isotopic profile for the entire section, in only a few of these was the matrix drilled for the isotopic profile. In the conglomerate samples, at least 2 clasts were drilled, as was the matrix, in at least two places for each sample. Several thin sections were made of conglomerates to complement the hand samples and to help us examine microfacies. Powder was collected and analyzed for  $\delta^{13}\text{C}_{\text{carb}}$  and  $\delta^{18}\text{O}_{\text{carb}}$  values using a Finnigan Delta XL + isotope ratio mass spectrometer with an automated carbonate prep system (Kiel III) at Stephen Burns' stable isotope laboratory at the University of Massachusetts, Amherst. Results are reported as the per mil difference between sample and the VPDB standard in delta notation where  $\delta^{18}\text{O}$  or  $\delta^{13}\text{C} = (\text{R}_{\text{sample}} / \text{R}_{\text{standard}} - 1) * 1000$ , and R is the ratio of the minor to the major isotope. Reproducibility of standard materials is 0.1‰ for  $\delta^{18}\text{O}$  and 0.05‰ for  $\delta^{13}\text{C}$ .

Finally, to investigate the role of diagenetic alteration in these samples, a subset of 236 samples was analyzed for trace element concentrations. A few samples were excluded from this analysis either because too little material was available from them or they were deemed inappropriate. Samples were prepared for inductively coupled plasma optical emission spectrometry (ICP-OES) on an Optima 7300DV ICP-OES (PerkinElmer Inc., Waltham, Massachusetts, USA) at Washington University. Approximately 1.0 mg of carbonate powder was dissolved in 10% (Optima grade) acetic acid in 15 mL Falcon centrifuge tubes. Samples were placed on a shaker table and left to dissolve overnight (~12 h). Samples were filtered through a 0.2 mm nylon filter prior to analysis.

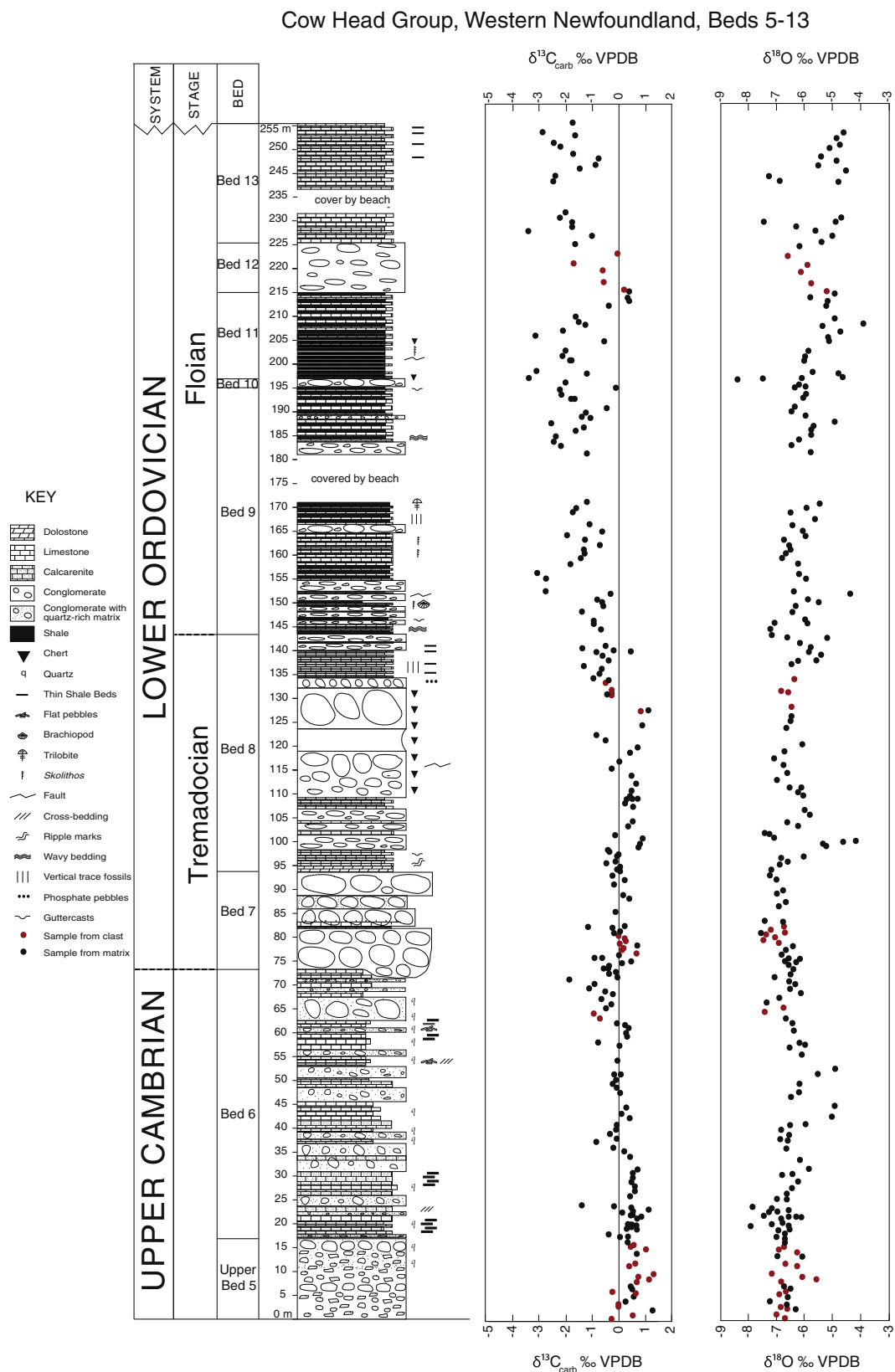


**Fig. 4.** The stratigraphic column of the Cow Head Group at the Cow Head Peninsula and its  $\delta^{13}\text{C}_{\text{carb}}$  and  $\delta^{18}\text{O}_{\text{carb}}$  profile. Values of  $\delta^{13}\text{C}$  are reported relative to Vienna PeeDee Belemnite standard. Note that black circles represent values measured from matrix samples, and red circles were derived from clasts of conglomerates. Age interpretations modified from James and Stevens (1986), but also see Fig. 2 for biostratigraphic constraints.

## 4. Results

### 4.1. Field and sample analysis

Facies, particularly the conglomerates, differ between these beds and suggest both large-scale and small-scale (local) processes sourced material for conglomerates and that the relative contribution of these processes varied across stratigraphy. Bed 5 is a large conglomerate-dominated bed (Fig. 4) that is exposed in a series of fault blocks along the Cow Head Peninsula. At least some of the clasts appear to be derived from in situ disrupted thin beds (Fig. 3A), which can sometimes be traced laterally over small distances ( $<1$  m). This suggests smaller-scale, localized disturbance in this environment and that at least some of these clasts are locally derived. In overlying Bed 6, facies were predominantly thinly-bedded ribbon limestone and calcarenous interbeds with shale. Conglomerates of this unit often contain rounded coarse quartz sand grains with micrite in the matrices visible in hand sample and thin section (Fig. 5). Conglomerates in this unit are lenticular and also appear to contain clasts derived from nearby thin-bedded limestone facies. Bed 7 is composed of four separate welded conglomerate beds. Conglomerates contain massive, white, boulder-sized clasts. The matrix of these conglomerates is not quartz-rich but rather dominated by small micritic clasts and fossil debris visible in thin section (Fig. 5). Bed 8 consists of dolostone, thinly bedded limestone, and massive chert-rich conglomerates. Thinly bedded limestone with guttercasts and wavy bedding is predominant near the base of the section and interspersed with conglomerate lenses. Much of the unit consists of massive conglomerates that vary in thickness laterally. The uppermost conglomerate contains phosphatic pebbles and the upper 10 m is marked by a return to thinly bedded limestone interspersed with shale. Conglomerates of Bed 8 are often recrystallized but, when well preserved, contain micritic matrices and rounded intraclasts in thin section (Fig. 5). Bed 9 is composed primarily of alternating beds of limestone and shale with occasional 1 to 5-meter-thick conglomerates. These conglomerates also contain a micritic or sparry cement-rich matrix. Bed 10 consists of a massive conglomerate that is approximately 1.7-meters-thick, though thickness varies along strike. Clasts

can be as large as boulder-sized. Matrix is largely recrystallized or micritic. Bed 12 is a 10-m-thick conglomerate bed that overlies the thin dolomitized beds of Bed 11. The conglomerate's matrix is composed primarily of calcareous shale and small limestone clasts, and more than two-thirds of the bed contains clasts on the scale of 0.5 m or larger (e.g., James and Stevens, 1986). The nature of conglomerates, including their clast size and matrix composition, varies significantly between and even within beds.

### 4.2. Carbon and oxygen isotope profile, Bed 5 through Bed 13, Cow Head Group

Carbon isotope data reveal stratigraphic trends, superimposed upon which there is bed-specific variability associated with the different facies and depositional environments of the Cow Head strata (Figs. 4 and 6). It is also important to note that some data points in the isotopic profile came from clasts of large conglomerate beds because the matrix could not be sampled in these areas (Fig. 4). Carbon isotope values are relatively heavy (0 to 1‰) in Bed 5 and the lower half of Bed 6. Values decrease in upper Bed 6 and lower Bed 7 (reaching  $-2\text{\textperthousand}$ ). Bed 8 values hover around 0‰ and become gradually more  $^{13}\text{C}$ -depleted into lower Bed 9 (with a nadir of  $\sim -2.5\text{\textperthousand}$ ).  $\delta^{13}\text{C}_{\text{carb}}$  variability increases above the covered portion of Bed 9, scatter increases in the values, with carbon isotope values oscillating between 0 and  $-4\text{\textperthousand}$  for the remainder of the section (upper Bed 9 through Bed 13, Fig. 4). While the scatter observed in data throughout the profile likely represents local processes that match the variability seen in individual conglomerate samples, the overall profile reflects a general trend from  $\sim +1\text{\textperthousand}$  at the base of the section to  $-2\text{\textperthousand}$  at the top (Fig. 4).

Parallel  $\delta^{18}\text{O}_{\text{carb}}$  measurements provide context for understanding processes during lithification and diagenesis. Oxygen isotopes show less scatter near the base of the column than near the top (Fig. 4). Values hover between  $-7\text{\textperthousand}$  and  $-5\text{\textperthousand}$  through Bed 7 and then show a positive excursion to heavier values (from  $-7\text{\textperthousand}$  to  $-4\text{\textperthousand}$ ) at the base of Bed 8, associated with a series of distinct dolomitized marker beds. Above this, values return to  $-7\text{\textperthousand}$  but variability increases in upper Bed 8 and through Bed 13 (Fig. 4).

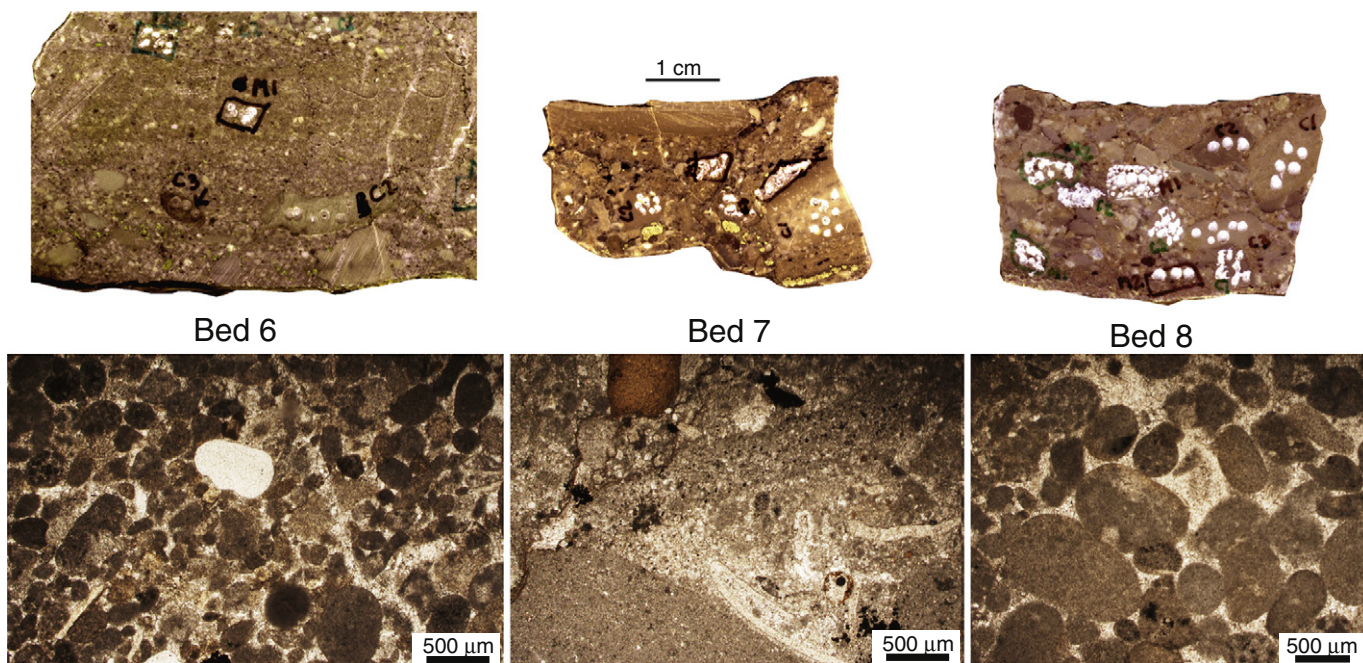
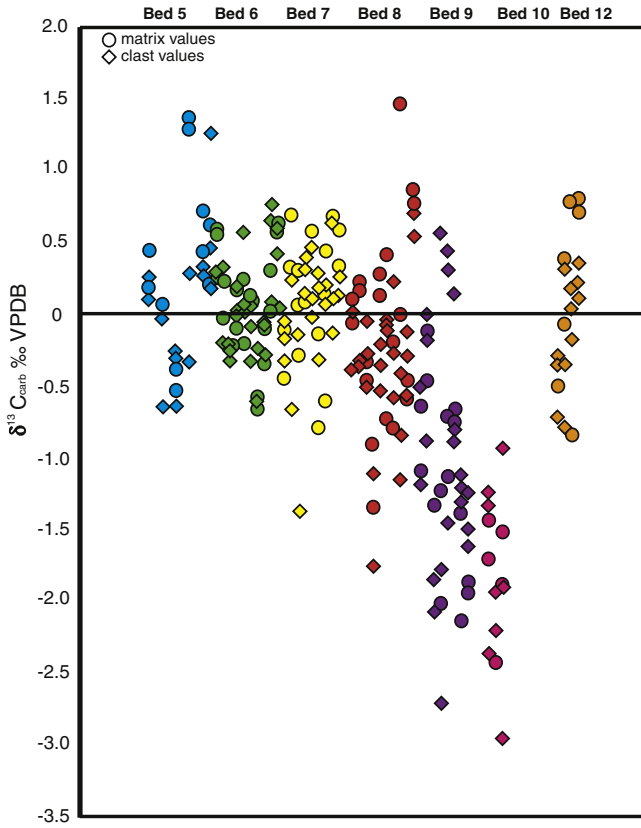


**Fig. 5.** Diagram showing polished faces of 3 representative samples from conglomeratic beds and their complementary thin sections. These polished samples show sites that were drilled for carbon isotope analysis of conglomerates, and thin sections show nature of clast and matrix. Note variability of clast composition and size. Notable features in thin section include round quartz grain of Bed 6, trilobite fossil of Bed 7, and micritic round intraclasts of Bed 8.

A



B

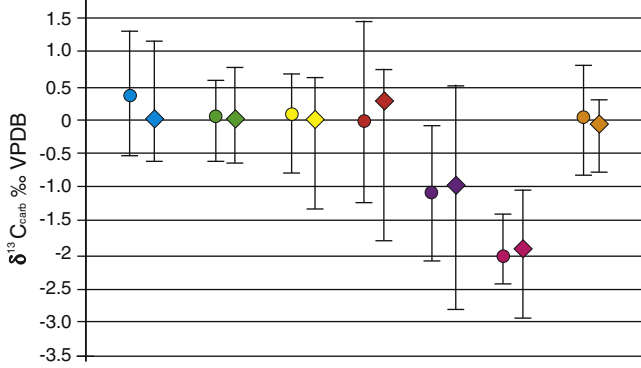


**Fig. 6.** Carbon isotope data for the clast and matrix values for 51 conglomerate samples. A) Diagram showing all data from the 51 samples. Each aligned set of values represents clast and matrix values measured from a single hand sample. B) Diagram showing the range and mean from all matrix and clast values measured in a single bed. Note that Bed 6 shows close alignment of the mean and ranges of clast and matrix values whereas Bed 9, though overlapping, has a much larger range of clast values than matrix values.

#### 4.3. Carbon isotope analysis of conglomerates

The  $\delta^{13}\text{C}_{\text{carb}}$  values of individual microfacies within conglomerate samples that span Bed 5 through Bed 13 reveal important differences between clast and matrix values (Fig. 6). (All standard deviations reported here for means are 1-sigma values.) In Bed 5, matrix values tend to cluster together and show no more than a 0.5% difference between values within a single sample (mean for all samples is  $0.40 \pm 0.59\text{\textperthousand}$ , Fig. 6). In contrast, clasts exhibit as much as a 1% spread in their values within a single sample (Fig. 6A). In contrast, Bed 6 shows a tight clustering of values (Fig. 6A, B). Although individual

samples show a range of isotopic values, this range is typically less than 1% (mean for matrix is  $0.07\text{\textperthousand}$  and  $0.04\text{\textperthousand}$  for clasts;  $\pm 0.34\text{\textperthousand}$  and  $0.36\text{\textperthousand}$ , respectively), and clast and matrix ranges overlap each other. In Bed 6, all values fall between  $-0.65\text{\textperthousand}$  and  $0.77\text{\textperthousand}$ , which is the smallest range of all beds examined (Fig. 6B). In Bed 7, the overall range of values is similar to Bed 6 with one outlier, but individual samples show greater scatter in both matrix and clast values (mean  $0.13\text{\textperthousand}$  for matrix  $\pm 0.45\text{\textperthousand}$ ,  $0.02\text{\textperthousand}$  for clast  $\pm 0.41\text{\textperthousand}$  (Fig. 6A, B). Overlying Bed 8 samples show the largest within-bed range of values, from  $-1.76\text{\textperthousand}$  to  $1.5\text{\textperthousand}$  (Fig. 6B). Individual samples can show as much as a 2% range (Fig. 6A); matrix values show as much as  $1.5\text{\textperthousand}$  variation (mean is  $-0.05 \pm 0.67\text{\textperthousand}$ ) whereas clast values exhibit less than 1% variation in a single sample (mean is  $-0.35 \pm 0.50\text{\textperthousand}$ ) (Fig. 6A). Bed 9 also exhibits large variability in clast and matrix values, with a total range of  $-2.7\text{\textperthousand}$  to  $0.6\text{\textperthousand}$ . Here, in general, clast values (mean is  $-1.17 \pm 0.61\text{\textperthousand}$ ) and matrix values (mean is  $-0.96 \pm 0.93\text{\textperthousand}$ ) show a large range (Fig. 6B). Beds 10 and 12 show a narrower range of values in all samples than Beds 8 and 9, and the values of individual samples have a range of about 1%. The mean for Bed 10 matrix and clast samples respectively is  $-1.98 \pm 0.44\text{\textperthousand}$  and  $-1.85 \pm 0.72\text{\textperthousand}$ . Bed 12 shows a return to more positive values, with a matrix mean of  $0.09 \pm 0.66\text{\textperthousand}$  and a clast mean of  $-0.12 \pm 0.39\text{\textperthousand}$ . Even so, matrix and clast values often do not overlap in individual samples from Beds 10 and 12 (Fig. 6).

#### 4.4. Carbon and oxygen isotope crossplots and trace element analyses

Carbon and oxygen isotope crossplots are constructed to assess the role of late-stage meteoric diagenesis in the measured values of ancient limestone. A potential feature of values altered as a result of this kind of diagenesis is a narrow range of oxygen isotope values coupled with a wide range of carbon isotope values (e.g., Allan and Matthews, 1977). A fingerprint of mixing zone alteration is a linear relationship between carbon and oxygen isotope values (Allan and Matthews, 1982). Carbon and oxygen crossplots for the profile of the Cow Head Group ( $R^2 = 0.09$ ) and for the conglomerate samples analyzed in this study ( $R^2$  value for clasts =  $0.10$ ;  $R^2 = 0.00$  value for matrix) are shown in Fig. 7A and B. In general, no linear relationship is revealed between carbon and oxygen isotope values in either subset, although a narrow range of oxygen isotope values does exist for these samples (e.g., Algeo et al., 1992), suggesting some burial diagenesis.

An analysis of carbon isotopes and trace element concentrations such as manganese (Mn), strontium (Sr) and iron (Fe) were also provided to examine the importance of late-stage diagenesis in these samples (Fig. 7C-E) (e.g., Pingitore, 1978; Banner and Hanson, 1990; Banner, 1995). No strong correlation exists for any trace element concentrations and carbon isotope values reported here (Fig. 7). Of note is that Sr concentrations are low for most samples, with only a few showing concentrations nearing 1000 ppm, but these samples do not co-vary with carbon isotope values.

## 5. Discussion

### 5.1. Diagenesis and Cow Head samples

The Cow Head Group of western Newfoundland is a deep-water section that preserves episodic deposition of transported shallow water material to the deep ocean (Coniglio and James, 1990) punctuated by background sedimentation in a deep-water environment. In addition to its complex depositional history, the unit has clearly experienced a combination of early and later stage diagenesis (e.g., Coniglio and James, 1988), all of which can affect the reliability of interpreting carbon isotope values as primary signals of seawater. Petrographic analysis of some Cow Head conglomerate samples reveals that many of these samples are well preserved, showing minimal dolomitization and an absence of abundant diagenetic cements. In addition, the trace element

## $\delta^{13}\text{C}$ vs $\delta^{18}\text{O}$ Values and Trace Element Data Beds 5–13, Cow Head Group

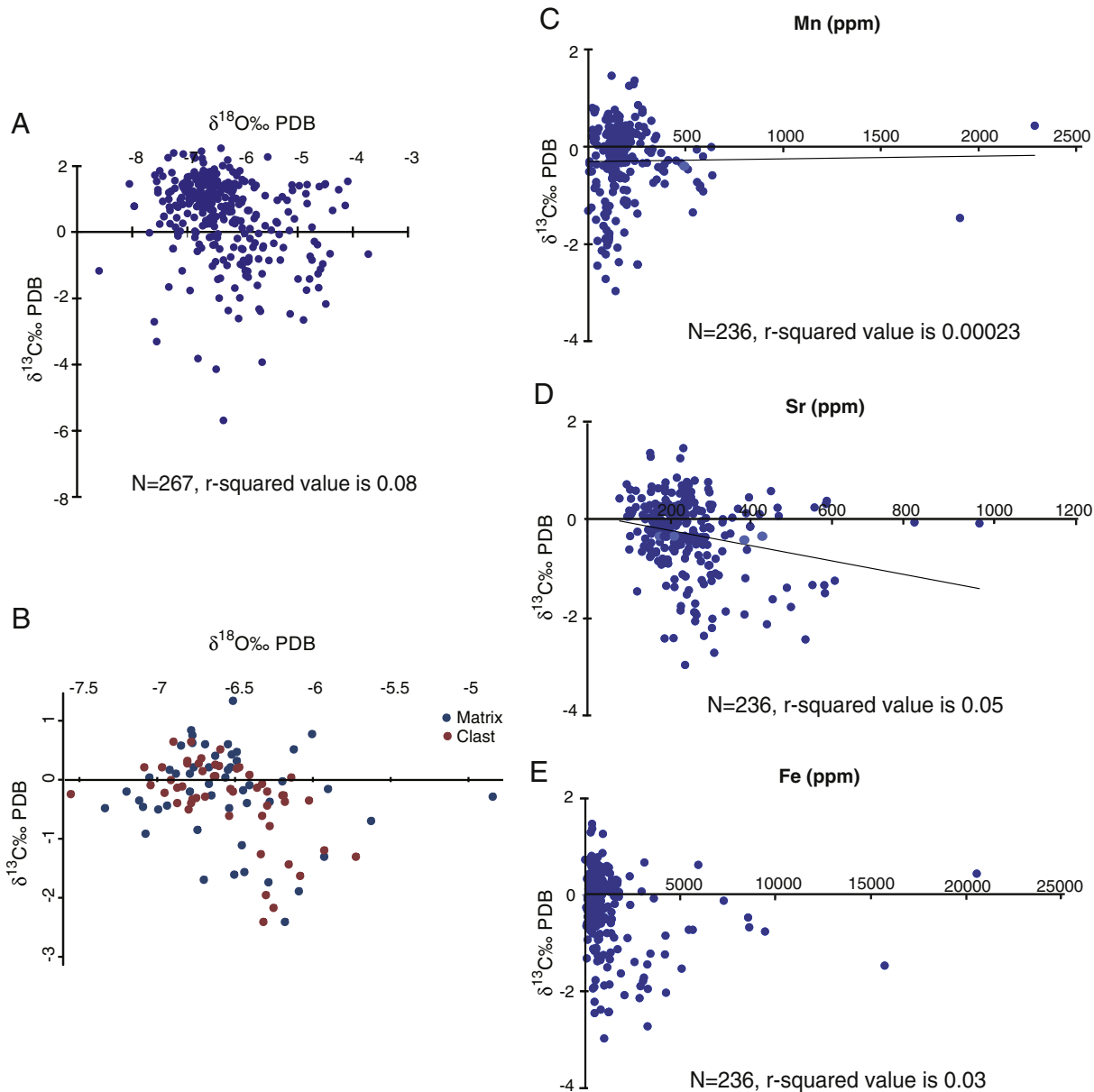


**Fig. 7.** Carbon and oxygen crossplots and crossplots of carbon with manganese, strontium, and iron concentrations. A) All carbon and oxygen isotope samples analyzed for the isotopic profiles of the Cow Head Group ( $R^2$  value = 0.09, slope is  $-0.1831x - 6.4182$ ); B) Carbon and oxygen isotopes from conglomerate samples analyzed, including matrix and clast values ( $R^2$  value for clasts = 0.10; slope is  $-0.1805x - 6.5893$ ;  $R^2$  = 0.00 value for matrix, slope is  $-0.0354x - 6.5647$ ); C) Carbon isotopes and manganese concentrations ( $R^2$  value = .00023; slope is  $6^{-5}x - 0.2994$ ); D) Carbon isotopes and strontium concentrations ( $R^2$  value = 0.05, slope is  $-0.0016x + 0.1017$ ); E) Carbon isotopes and iron concentrations ( $R^2$  value = 0.03, slope is  $y = -7^{-5}x - 0.2094$ ).

concentrations of all samples do not covary with carbon isotope values (Fig. 7), suggesting the variable depletion in carbon isotopic composition was acquired independent of reducing fluids that would have generated enrichments in redox-sensitive metals. The narrow range of oxygen isotopes suggests that these rocks experienced at least some late stage burial diagenesis (Algeo et al., 1992), but some primary signal is retained in these data. The lack of covariation between  $\delta^{13}\text{C}$  and  $\delta^{18}\text{O}$  data suggests that the origin of the  $\delta^{13}\text{C}$  variability was not the result of meteoric diagenesis with both  $^{13}\text{C}$ -depleted and  $^{18}\text{O}$ -depleted fluids. What is important to note is that the complexity of this depositional package – one in which some parts of the section are dominated by allochthonous carbonate that may have been transported long distances

from shallower water settings (e.g., Beds 7 and 8) – will play a role in the way in which carbon isotopes are preserved in conglomeratic samples. However, in the construction of the carbon isotope profile, care was taken to avoid conglomerate samples where possible, to maximize meaningful stratigraphic isotopic information.

### 5.2. The carbon isotope profile, Beds 5 through 13 of the Cow Head Group

The carbon isotope profile of Beds 5 through 13 show broad scale changes from the upper Cambrian to the Lower Ordovician, with some additional scatter superimposed on these trends that likely relates to diagenesis (Fig. 4). This section is highly condensed relative to other

Cambro-Ordovician sections worldwide (e.g., Great Basin strata are >4 km-thick; Derby et al., 2012); however, as in at least a few other sections, these data reveal a trend of more positive values in the middle and later Cambrian followed by more negative values in the Ordovician (e.g., Saltzman and Thomas, 2012; Buggisch et al., 2003, Fig. 8). Although, these data show some agreement with those of other areas such as the Argentina pre-Cordillera and western US (Buggisch et al., 2003; Saltzman and Thomas, 2012), some notable exceptions exist. Firstly, the SPICE event is missing in the deep water Cow Head section despite its presence in nearby shelf equivalents (Saltzman et al., 2004; Hurtgen et al., 2009). The absence of SPICE is important to note in these sections because its absence suggests a number of possibilities. One is that the SPICE event may be highly condensed in these deep-water sections, as the biostratigraphy suggests, and therefore may not be well preserved (Westrop and Eoff, 2012). Another possibility is that the SPICE is not expressed in these deep-water sections. Third, it is possible that the SPICE event is preserved at Cow Head but was not sampled in this work. Although we cannot be sure why the SPICE event was not found during this research, fossils assemblages support the first possibility.

In addition to the absence of the SPICE event, there is difficulty in identifying the Cambro-Ordovician boundary within the conglomeratic Cow Head Group facies, despite its close proximity to the GSSP for this boundary at Green Point (e.g., Cooper et al., 2001; Azmy et al., 2014). This uncertainty may result in some misalignment with global data. In general, our carbon isotope profile shows a shift from positive values in the latest Cambrian to more negative values in the lowermost Ordovician, much like the global profile (Fig. 8). Both profiles show a small shift toward positive values within the mid-Tremadocian and

then remain mostly negative for the remainder of the Lower Ordovician. It is worth noting that the Cow Head strata show significant scatter through the Floian, which is different from the Argentinian sections (Buggisch et al., 2003) and global compilation (Bergstrom et al., 2008). For example, the Cow Head does not record a return to more positive values in the later Floian as in these other sections, and the conodonts, particularly *Lenodus variabilis*, suggest a late Early to early Middle Ordovician age. It is possible that the lack of correlation in isotopes this section is related to early diagenetic processes in Beds 9 through 13 (see below).

### 5.3. Carbon isotopes of conglomerates of the Cow Head Group

Substantial variability (~4.5‰) exists in the  $\delta^{13}\text{C}_{\text{carb}}$  of the matrix and clasts of the conglomerate beds that make up the Cow Head Group (Fig. 6). While a fraction of this can be ascribed to stratigraphic variability, there are many cases where the within-bed variability is in excess of 2‰. This level of variability can exist between different clasts in the same bed, between different portions of matrix within the same bed, and between clasts and matrix within the same bed. It is also important to note that the variability within beds, which are broadly defined lithostratigraphically, may also reflect the source of carbonate and variable diagenetic processes in these units. For example, Bed 6 consists of small-scale, meter-sized conglomerate beds with clasts that appear to be locally sourced (Fig. 3A). In contrast, Beds 7 and 8 contain massive decameter-scale conglomerates with boulder-sized clasts sourced from the nearby slope (Fig. 3B; e.g., Coniglio and James, 1985). These different conglomerates of Beds 6, 7 and 8 also show very different isotopic variability (Fig. 6), which may in part reflect the ways in which

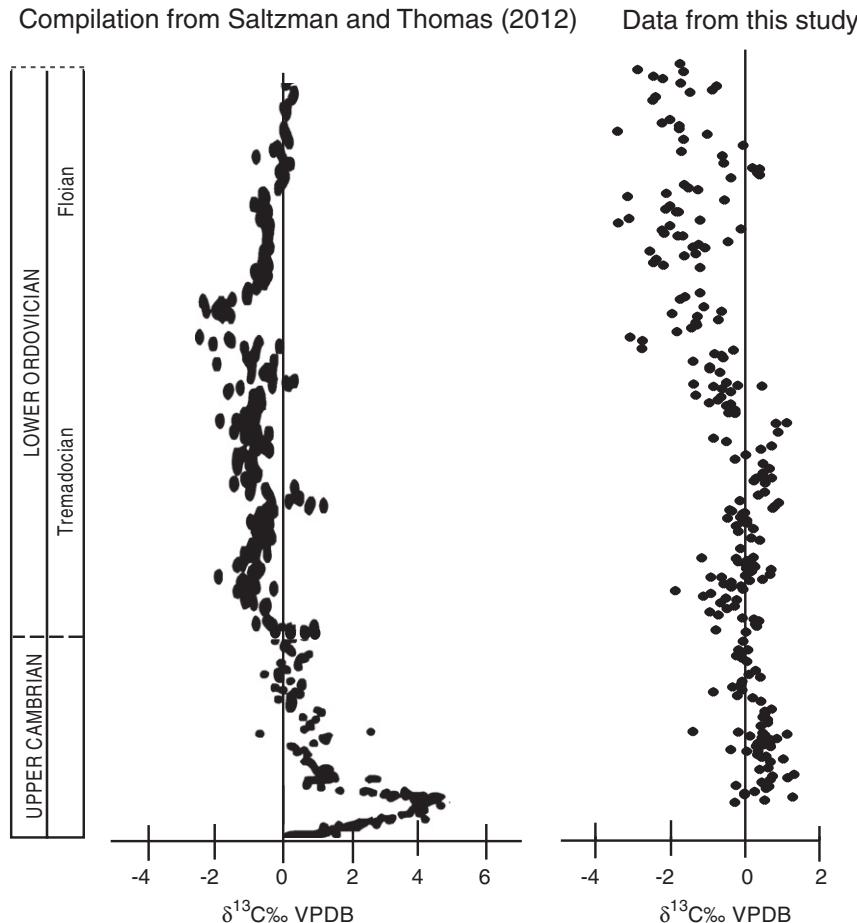


**Fig. 8.** Composite carbon isotope profile from Saltzman and Thomas (2012) and references therein (A) and profile from this work (B).

these units were deposited. While this observation does not directly inform the origin of the variability in these different beds, it suggests that not all conglomerates, even those within the same broad depositional environment, may be expected to record the same processes (Husson et al., 2012).

The variability seen within each bed, particularly in matrix values, may be related to several processes. First, it could reflect primary variability in water column chemistry (either temporally or spatially). However, the high frequency variations make it hard to reconcile the observed variability as the result of temporal changes in open marine water column  $\delta^{13}\text{C}$ . Similarly, the variable composition of the clasts, and the changing offsets between clasts and matrix (sometimes clasts are  $^{13}\text{C}$ -enriched and sometimes they are  $^{13}\text{C}$ -depleted relative to the matrix) make a constant lateral gradient in water column  $\delta^{13}\text{C}$  hard to reconcile with the observed patterns.

A second explanation for the observed variability could be the influence of differing amounts of late-stage diagenesis among the samples. In this case, samples with more diagenetic alteration would be expected to have more  $^{13}\text{C}$ -depleted signatures. However, we observe no covariation between  $\delta^{13}\text{C}_{\text{carb}}$  and  $\delta^{18}\text{O}_{\text{carb}}$  or Sr, Mn or Fe concentrations (Fig. 7) as would be expected by diagenetic overprinting. Further, if diagenetic alteration were the cause of the observed isotopic variability, patterns in  $\delta^{13}\text{C}$  would be expected to track lithology (e.g., reflecting the porosity and permeability of the samples). No such patterns are observed (i.e., sometimes matrix is  $^{13}\text{C}$ -enriched relative to clasts and sometimes  $^{13}\text{C}$ -depleted, with no correlation based on lithofacies).

An alternative explanation is that the observed variability reflects the local conditions in porewaters during lithification. Here, a  $^{13}\text{C}$ -depleted signal could reflect a contribution of authigenic carbonates forming early marine cements with porewater  $\delta^{13}\text{C}_{\text{DIC}}$  lower than coeval seawater. The resulting  $\delta^{13}\text{C}_{\text{carb}}$  signal could be lower as a function of the amount of authigenic early marine cement (lowering the  $\delta^{13}\text{C}_{\text{carb}}$ ) and/or the isotopic composition of the local porewater  $\delta^{13}\text{C}_{\text{DIC}}$  pool. This DIC pool would have lowered  $\delta^{13}\text{C}_{\text{carb}}$  as the result of microbial respiration (aerobic and/or anaerobic). Anaerobic metabolisms (e.g., sulfate reduction) in particular increase alkalinity and drive carbonate precipitation (e.g., Bosak and Newman, 2003). All things being equal, sediments with higher organic carbon contents can generate more  $^{13}\text{C}$ -depleted DIC and therefore carbonates with lower  $\delta^{13}\text{C}_{\text{carb}}$  values.

If this interpretation is correct, it suggests that clasts in the Cow Head conglomerates were sourced from a variety of both autochthonous and upslope environments that varied strongly in their local organic carbon loading, leading to variable depletions in  $\delta^{13}\text{C}_{\text{carb}}$  of these early-lithified clasts. As the biostratigraphy of these sections suggest, clasts are often derived from strata that are older but do not significantly predate deposition in these deep water sections (Zhang and Barnes, 2004; Westrop and Eoff, 2012; Westrop and Dengler, 2014). Our data suggest that variation in the organic carbon contents in the matrix and therefore in early diagenetic remineralization (possibly recorded as variable fractions of authigenic allochthonous carbonate in the matrix) was the cause for these offsets in  $\delta^{13}\text{C}_{\text{carb}}$  of the matrix relative to the clasts (e.g., Kump and Arthur, 1999; Metzger and Fike, 2013). These data suggest that local variations in organic carbon loading during deposition and associated microbial respiration during early lithification can imprint the resulting isotopic signature preserved in marine carbonates. The resulting  $\delta^{13}\text{C}_{\text{carb}}$  overprints can explain much of the isotopic spatial (lateral) and temporal (stratigraphic) variability observed in many chemostratigraphic records, particularly those found in Cambrian strata (e.g., Coniglio, 1989; Maloof et al., 2005; 2010; Saltzman et al., 1998; 2000).

In spite of the variability recorded in individual conglomerate samples, a general trend can be gleaned that still matches the broad scale progression of the carbon isotope profile as a whole. The  $\delta^{13}\text{C}_{\text{carb}}$  values show spread that varies from bed to bed, but even so, the general trend moves from more positive values in the later Cambrian Beds 5 and 6 to

more negative values in Lower Ordovician Bed 9 upwards. This demonstrates that even with local processes governing the carbon isotope signal of individual drilled samples, information about the water column can be retained when examining samples en masse as we have done here.

## 6. Conclusions

Our record of the evolution of carbon cycling over Earth history comes primarily from shallow-water carbonates. Here we present a Cambro-Ordovician record of  $\delta^{13}\text{C}_{\text{carb}}$  variability from the Cow Head Group strata deposited in a slope-basinal environment. The resulting deep-water  $\delta^{13}\text{C}_{\text{carb}}$  curve matches the global record, albeit with substantial scatter (up to ~2‰) superimposed upon it. This enhanced  $\delta^{13}\text{C}_{\text{carb}}$  variability is not the result of later-stage meteoric diagenesis, but reflects the contribution of multiple pulses of carbonate precipitation in these samples, each associated with local DIC reservoirs variably impacted by microbial respiration of organic matter. These data indicate that post-depositional processes, such as local organic matter remineralization and early authigenic carbonate precipitation during lithification, play a dominant role in controlling  $\delta^{13}\text{C}_{\text{carb}}$  values in Cambrian carbonates, an interval of time that may have experienced fluctuating redox perhaps more so than other intervals of Earth history.

## Acknowledgments

SBP would like to acknowledge A. Breus, H. Clemente, M. Laflamme, and M. Rolls for field assistance and Smith College for funding. We also gratefully acknowledge helpful reviews from 2 reviewers and the editor that improved this manuscript.

## References

- Algeo, T.J., Wilkinson, B.H., Kyger, C.L., 1992. Meteoric-burial diagenesis of Middle Pennsylvanian limestones in the Orogenome Basin, New Mexico: water/rock interactions and basin geothermics. *J. Sediment. Petrol.* 62, 652–670.
- Allan, J.R., Matthews, R.K., 1977. Carbon and oxygen isotopes as diagenetic and stratigraphic tools: data from surface and subsurface Barbados, West Indies. *Geology* 5, 16–20.
- Allan, J.R., Matthews, R.K., 1982. Isotope signatures associated with early meteoric diagenesis. *Sedimentology* 29, 797–817.
- Arthur, M.A., Dean, W.E., Pratt, L.M., 1988. Geochemical and climatic effects of increased marine organic carbon burial at the Cenomanian/Turonian boundary. *Nature* 335, 714–717.
- Azmy, K., Souge, S., Brand, U., Bagnoli, G., Ripperdan, R., 2014. High-resolution chemostratigraphy of the Cambrian–Ordovician GSSP: enhanced global correlation tool. *Palaeogeogr. Palaeoclimatol. Palaeoecol.* 409, 135–144.
- Banner, J.L., 1995. Application of the trace element and isotope geochemistry of strontium to studies of carbonate diagenesis. *Sedimentology* 42, 805–824.
- Banner, J.L., Hanson, G.N., 1990. Calculation of simultaneous isotopic and trace element variations during water–rock interaction with applications to carbonate diagenesis. *Geochim. Cosmochim. Acta* 54, 3123–3137.
- Barnes, C.R., 1988. The proposed Cambrian–Ordovician Global Boundary Stratotype and Point (GSSP) in Western Newfoundland, Canada. *Geol. Mag.* 125, 381–414.
- Bergstrom, S.M., Chen, X., Gutierrez-Marcos, J.C., Dronov, A., 2008. The new chronostratigraphic classification of the Ordovician System and its relations to major regional series and stages and to  $\delta^{13}\text{C}$  chemostratigraphy. *Lethaia* 42, 97–107.
- Bosak, T., Newman, D.K., 2003. Microbial nucleation of calcium carbonate in the Precambrian. *Geology* 31, 577–580.
- Buggisch, W., Keller, M., Lehnert, O., 2003. Carbon isotope record of Late Cambrian to Early Ordovician carbonates of the Argentine Precordillera. *Palaeogeogr. Palaeoclimatol. Palaeoecol.* 195, 357–373.
- Chow, N., James, N.P., 1987. Cambrian grand cycles: a northern Appalachian perspective. *Geol. Soc. Am. Bull.* 98, 418–429.
- Coniglio, M., 1989. Neomorphism and cementation in ancient deep-water limestones, Cow Head Group (Cambro-Ordovician), western Newfoundland, Canada. *Sediment. Geol.* 65, 15–33.
- Coniglio, James, 1985. Calcified algae as sediment contributors to Early Paleozoic limestones: evidence from deep-water sediments of the Cow Head Group, Western Newfoundland. *J. Sediment. Res.* 55, 746–754.
- Coniglio, M., James, N., 1990. Origin of fine-grained carbonate and siliciclastic sediments in an early Paleozoic slope sequence, Cow Head Group, western Newfoundland. *Sedimentology* 37, 215–230.
- Cooper, R.A., Nowlan, G.S., Williams, S.H., 2001. Global stratotype section and point for base of the Ordovician system. *Episodes* 24, 19–28.

- Cowan, C.A., James, N.P., 1993. The interactions of sea-level change, terrigenous-sediment influx, and carbonate productivity as controls on Upper Cambrian grand cycles of western Newfoundland, Canada. *Geol. Soc. Am. Bull.* 105, 1576–1590.
- Derby, James R., Raine, Robert J., Runkel, Anthony C., Paul Smith, M., 2012. Paleogeography of the great American carbonate bank of Laurentia in the earliest Ordovician (early Tremadocian): the Stonehenge transgression. In: Derby, J.R., Fritz, R.D., Longacre, S.A., Morgan, W.A., Sternbach, C.A. (Eds.), *The great American carbonate bank: The geology and economic resources of the Cambrian–Ordovician Sauk megasequence of Laurentia*. AAPG Memoir vol. 98, pp. 5–13.
- Droser, M.L., Finnegan, S., 2003. The Ordovician radiation: a follow-up to the Cambrian explosion? *J. Integr. Comp. Biol.* 43, 178–184.
- Freeman, K.H., Hayes, J.M., 1992. Fractionation of carbon isotopes by phytoplankton and estimates of ancient  $\text{CO}_2$  levels. *Glob. Biogeochem. Cycles* 6, 185–198.
- Grotzinger, J.P., Fike, D.A., Fischer, W.W., 2011. Enigmatic origin of the largest-known carbon isotope excursion in Earth's history. *Nat. Geosci.* 4, 285–291.
- Hayes, J.M., Strauss, H., Kaufman, A.J., 1999. The abundance of  $^{13}\text{C}$  in marine organic matter and isotopic fractionation in the global biogeochemical cycle of carbon during the past 800 Ma. *Chem. Geol.* 161, 103–125.
- Hurtgen, M.T., Pruss, S.B., Knoll, A.H., 2009. Evaluating the relationship between the carbon and sulfur cycles in the later Cambrian ocean; an example from the Port Au Port group, western Newfoundland, Canada. *Earth Planet. Sci. Lett.* 281, 288–297.
- Husson, J.M., Maloof, A.C., Schoene, B., 2012. A syn-depositional age for Earth's deepest  $^{13}\text{C}$  excursion required by isotope conglominate tests. *Terra Nova* 24, 318–325.
- James, N.P., Stevens, R.K., 1986. Stratigraphy and correlation of the Cambro-Ordovician Cow Head Group, western Newfoundland. *Bull. Geol. Surv. Can.* 366 (143 pp.).
- Johnston, D., Barnes, C.R., 1999. Early and Middle Ordovician (Arenig) conodonts from St. Pauls Inlet and Martin Point, Cow Head Group, western Newfoundland, Canada. *Geol. Palaeontol.* 33, 21–70.
- Karim, T.S., 2008. Olenid-dominated trilobite fauna from the Shallow Bay Formation (Cow Head Group), Cambrian–Ordovician boundary interval, western Newfoundland. *Can. J. Earth Sci.* 45, 407–425.
- Knoll, A.H., Hayes, J.M., Kaufman, A.J., Swett, K., Lambert, I.B., 1986. Secular variation in carbon isotope ratios from upper Proterozoic successions of Svalbard and East Greenland. *Nature* 321, 832–838.
- Kump, L.R., Arthur, M.A., 1999. Interpreting carbon-isotope excursions: carbonates and organic matter. *Chem. Geol.* 161, 181–198.
- Maloof, A.C., Schrag, D.P., Crowley, J.L., Bowring, S.A., 2005. An expanded record of Early Cambrian carbon cycling from the Anti-Atlas Margin, Morocco. *Can. J. Earth Sci.* 42, 2195–2216.
- Maloof, A.C., Ramezani, J., Bowring, S.A., Fike, D.A., Porter, S.M., Mazouad, M., 2010. Constraints on early Cambrian carbon cycling from the duration of the Nemakit-Daldynian–Tommotian boundary  $^{13}\text{C}$  shift, Morocco. *Geology* 38, 623–626.
- Metzger, J.G., Fike, D.A., 2013. Techniques for assessing spatial heterogeneity of carbonate  $^{13}\text{C}$ : implications for craton-wide isotope gradients. *Sedimentology* 60 (6), 1405–1431.
- Oehlert, A.M., Swart, P.K., 2014. Interpreting carbonate and organic carbon isotope covariance in the sedimentary record. *Nat. Commun.* 5. <http://dx.doi.org/10.1038/ncomms5672>.
- Pingitore, N.E., 1978. The Behavior of  $\text{Zn}^{2+}$  and  $\text{Mn}^{2+}$  during carbonate diagenesis: Theory and applications. *J. Sediment. Petrol.* 48, 799–814.
- Popp, B.N., Takigiku, R., Hayes, J.M., Louda, J.W., Baker, E.W., 1989. The post-Paleozoic chronology and mechanism of  $^{13}\text{C}$  depletion in primary marine organic matter. *Am. J. Sci.* 289, 426–454.
- Sackett, W.M., 1991. A history of the  $\delta^{13}\text{C}$  composition of oceanic plankton. *Mar. Chem.* 34, 153–156.
- Saltzman, M.R., Thomas, E., 2012. Carbon isotope stratigraphy. In: Felix, M., Gradstein, F.M., Ogg, J.G., Schmitz, M., Ogg, G. (Eds.), *The Geologic Time Scale*, pp. 207–232. <http://dx.doi.org/10.1016/B978-0-444-59425-9.00011-1>.
- Saltzman, M.R., Runnegar, B., Lohmann, K.C., 1998. Carbon-isotope stratigraphy of the Pterocephalid Biome in the eastern Great Basin: record of a global oceanographic event during the Late Cambrian. *Geol. Soc. Am. Bull.* 110, 285–297.
- Saltzman, M.R., Brasier, M.D., Ripperdan, R.L., Ergaliev, G.K., Lohmann, K.C., Robison, R.A., Chang, W.T., Peng, S., Runnegar, B., 2000. A global carbon isotope excursion during the Late Cambrian: relation to trilobite extinctions, organic-matter burial and sea level. *Palaeogeogr. Palaeoclimatol. Palaeoecol.* 162, 211–224.
- Saltzman, M.R., Cowan, C.A., Runkel, A.C., Runnegar, B., Stewart, M.C., Palmer, A.R., 2004. The late Cambrian spice ( $^{13}\text{C}$ ) event and the SAUK II–SAUK III regression: new evidence from Laurentian basins in Utah, Iowa, and Newfoundland. *J. Sediment. Res.* 74, 366–377.
- Schrag, D.P., Higgins, J.A., Macdonald, F.A., Johnston, D.T., 2013. Authigenic carbonate and the history of the global carbon cycle. *Science* 339, 540–543.
- Suechecki, R.K., Hubert, J.F., 1984. Stable isotopic and elemental relationships of ancient shallow-marine and slope carbonates, Cambro-Ordovician Cow Head Group, Newfoundland: implications for fluid flux. *J. Sediment. Res.* 54, 1062–1080.
- Tripathy, G.R., Hannah, J.L., Stein, H.J., Yang, G., 2014. Re-Os age and depositional environment for black shales from the Cambrian–Ordovician boundary, Green Point, western Newfoundland. *Geochim. Geophys. Geosyst.* 15, 1021–1037. <http://dx.doi.org/10.1002/2013GC005217>.
- Westrop, S.R., Dengler, A.A., 2014. The mid-Cambrian (Series 3, Guzhangian; Marjuman) trilobite *Deiracephalus* Resser, 1935, from western Newfoundland. *Can. J. Earth Sci.* 51, 682–700.
- Westrop, S.R., Eoff, J.D., 2012. Late Cambrian (Furongian; Paibian, Steptoean) Agnostid arthropods from the Cow Head Group, western Newfoundland. *J. Paleontol.* 86, 201–237.
- Zhang, S., Barnes, C.R., 2004. Arenigian (Early Ordovician) sea-level history and the response of conodont communities, western Newfoundland. *Can. J. Earth Sci.* 41, 843–865.